Journal of Bioenergetics and Biomembranes, Vol. 25, No. 3, 1992

Minireview

Mutational Analysis of Assembly and Function of the Iron–Sulfur Protein of the Cytochrome bc_1 Complex in *Saccharomyces cerevisiae*

Laurie A. Graham,[1] Ulrich Brandt,[1] John S. Sargent,[1] and Bernard L. Trumpower[1]

Received December 16, 1992; accepted January 10, 1993

The iron–sulfur protein of the cytochrome bc_1 complex oxidizes ubiquinol at center P in the protonmotive Q cycle mechanism, transferring one electron to cytochrome c_1 and generating a low-potential ubisemiquinone anion which reduces the low-potential cytochrome *b*-566 heme group. In order to catalyze this divergent transfer of two reducing equivalents from ubiquinol, the iron–sulfur protein must be structurally integrated into the cytochrome bc_1 complex in a manner which facilitates electron transfer from the iron–sulfur cluster to cytochrome c_1 and generates a strongly reducing ubisemiquinone anion radical which is proximal to the *b*-566 heme group. This radical must also be sequestered from spurious reactivities with oxygen and other high-potential oxidants. Experimental approaches are described which are aimed at understanding how the iron–sulfur protein is inserted into center P, and how the iron–sulfur cluster is inserted into the apoprotein.

KEY WORDS: Rieske iron–sulfur protein, RIP1; *Saccharomyces cerevisiae*; mitochondria; bc_1 complex; QCR9; iron–sulfur cluster, mitochondrial targeting.

INTRODUCTION

The Rieske iron–sulfur protein is one of three redox proteins, the other two being cytochrome c_1 and the di-heme cytochrome *b*, which is an obligatory participant in the protonmotive electron transfer mechanism of the cytochrome bc_1 and cytochrome *bf* complexes in a wide variety of prokaryotic and eukaryotic species (Trumpower, 1990a). In all eukaryotes thus far examined, including both oxygenic and photosynthetic organisms, the Rieske protein is encoded on the nuclear genome and targeted to the energy-transducing membrane of the mitochondrion or chloroplast. In prokaryotes the protein is targeted from the cytoplasm to the cytoplasmic membrane. The details of how the Rieske protein is assembled into the membranous *bc* complex, when in the sequence of assembly the iron–sulfur cluster is inserted, what accessory proteins may be required for assembly of the protein, and how the iron–sulfur protein interacts with cytochrome c_1 and cytochrome *b* are questions which remain to be answered.

Earlier experiments on resolution and reconstitution of the iron–sulfur protein and establishment of the role of the iron–sulfur protein in the protonmotive *Q* cycle have been reviewed elsewhere (Trumpower, 1981, 1990b). In this review we will describe recent experiments which shed new light on how the iron–sulfur protein is assembled into the cytochrome bc_1 complex in *S. cerevisiae*, how the iron–sulfur cluster is inserted into the apoprotein, and how the structure of the protein has been conserved among various species.

[1] Department of Biochemistry, Dartmouth Medical School, Hanover, New Hampshire 03755.

0145-479X/93/0600-0245$07.00/0

CONSERVATION OF STRUCTURAL DOMAINS IN THE RIESKE IRON–SULFUR PROTEIN FROM PHYLOGENETICALLY DIVERSE SPECIES

The nuclear genes encoding the Rieske iron–sulfur protein have now been cloned and sequenced from 15 species, and from these the sequences of the proteins have been deduced. In Fig. 1 we have aligned the sequences of the mature iron–sulfur proteins. The N-terminal sequences and thus the sites of post-translational processing which generate the mature sized iron–sulfur protein are known from sequencing of the mature sized iron–sulfur proteins from *S. cerevisiae* (Ysc; Beckmann *et al.*, 1987), *N. crassa* (Ncr; Harnisch *et al.*, 1985), and bovine heart (Bov; Schägger *et al.*, 1987). The homologous N-termini of the mature iron–sulfur proteins can be deduced from the *c*DNA sequences for the iron–sulfur proteins from rat (Rat; Nishikimi *et al.*, 1989) and humans (Hum; Nishikimi *et al.*, 1990) by comparison of those amino acid sequences with that of the mature protein from bovine heart (Schägger *et al.*, 1987; Usui *et al.*, 1990). The N-terminal sequence of the mature bovine protein, SHTDIDVPDFS (Schägger *et al.*, 1987), appears in the N-terminal portion of the rat and human proteins at a location which fits the criteria for mitochondrial targeting and post-translational protease processing. The N-terminal sequence of the mature iron–sulfur protein from spinach chloroplasts (Sph; Steppuhn *et al.*, 1987) was established from the protein sequence.

The N-terminal sequences of the mature iron–sulfur proteins from tobacco mitochondria and corn mitochondria (Tob and Maz; Huang *et al.*, 1991) are not known, since the proteins have not been purified or sequenced from these species. We have deduced the probable N-terminal sequences of these mature proteins by examining their predicted secondary structures in the N-terminal portions of the full-length proteins for amphipathic helices, the conserved structural motifs which are associated with post-translational processing by mitochondrial proteases, and confirming the existence of a consensus amino acid sequence required for two-step processing by the mitochondrial proteases (Hendrick *et al.*, 1989) in the sequence of the maize iron–sulfur protein.

The genes for the Rieske iron–sulfur protein have also been sequenced from *R. rubrum* (Rrb; Majewski and Trebst, 1990), *R. viridis* (Rvr; Verbist *et al.*, 1989), *Bradyrhizobium japonicum* (Rhz; Thoeny-Meyer *et al.*, 1989); *P. denitrificans* (Pdn; Kurowski and Ludwig, 1987), *Rh. capsulatus* (Rcp; Davidson and Daldal, 1987), *Nostoc* (Nos; Kallas *et al.*, 1989), and *Synechococcus* (Widger, GenBank Accession No. M74514). It is generally assumed that the iron–sulfur proteins do not have cleaved targeting presequences in prokaryotes, and the predicted secondary structures at the N-termini of the full length bacterial proteins resemble the predicted secondary structures at the N-termini of the mature eukaryotic proteins. However, there has been very little protein chemistry performed to support this assumption. We have depicted the sequences of the mature bacterial proteins as beginning with the N-terminal methionine (Fig. 1), although in *R. rubrum* the N-terminal methionine was shown to be removed post-translationally (Majewski and Trebst, 1990).

On the basis of these sequences it is possible to construct a dendrogram of the type shown in Fig. 2. In this graphical representation the vertical distance between species is proportional to the extent of amino acid sequence homology. It is interesting to note that by this criterion the yeast protein is more closely related to the mammalian proteins than it is to the plant proteins. Similarly, the Rieske protein from *Rh. capsulatus* is more similar to that from *P. denitrificans* than it is to the proteins from *R. rubrum* or *R. viridis*. Also, the Rieske proteins from the nitrogen fixing and denitrifying bacteria are each more similar to the Rieske proteins from a photosynthetic bacterium than they are to each other.

In all of the iron–sulfur protein sequences thus far deduced, there are four conserved cysteines and two conserved histidines. The location of these within the predicted secondary structure of the iron–sulfur protein is shown in Fig. 3. It is now established that two histidines are ligands to the iron–sulfur cluster (Kuila *et al.*, 1987; Gurbiel *et al.*, 1989; Britt *et al.*, 1991), and it is likely that two of the conserved cysteines constitute the remaining ligand quartet. Since His-161 and His-181 are the only histidines conserved in all species (Fig. 1), and replacement of the extensively but not universally conserved His-184 (Fig. 1) with arginine did not impair iron–sulfur protein function (Table I and Graham and Trumpower, 1991), we conclude that His-161 and His-181 are two of the cluster ligands.

Which two of the four cysteines are iron ligands is not yet established with certainty. It seems unlikely, for steric reasons, that an iron atom could be liganded to Cys-180, if the second iron is liganded to His-181.

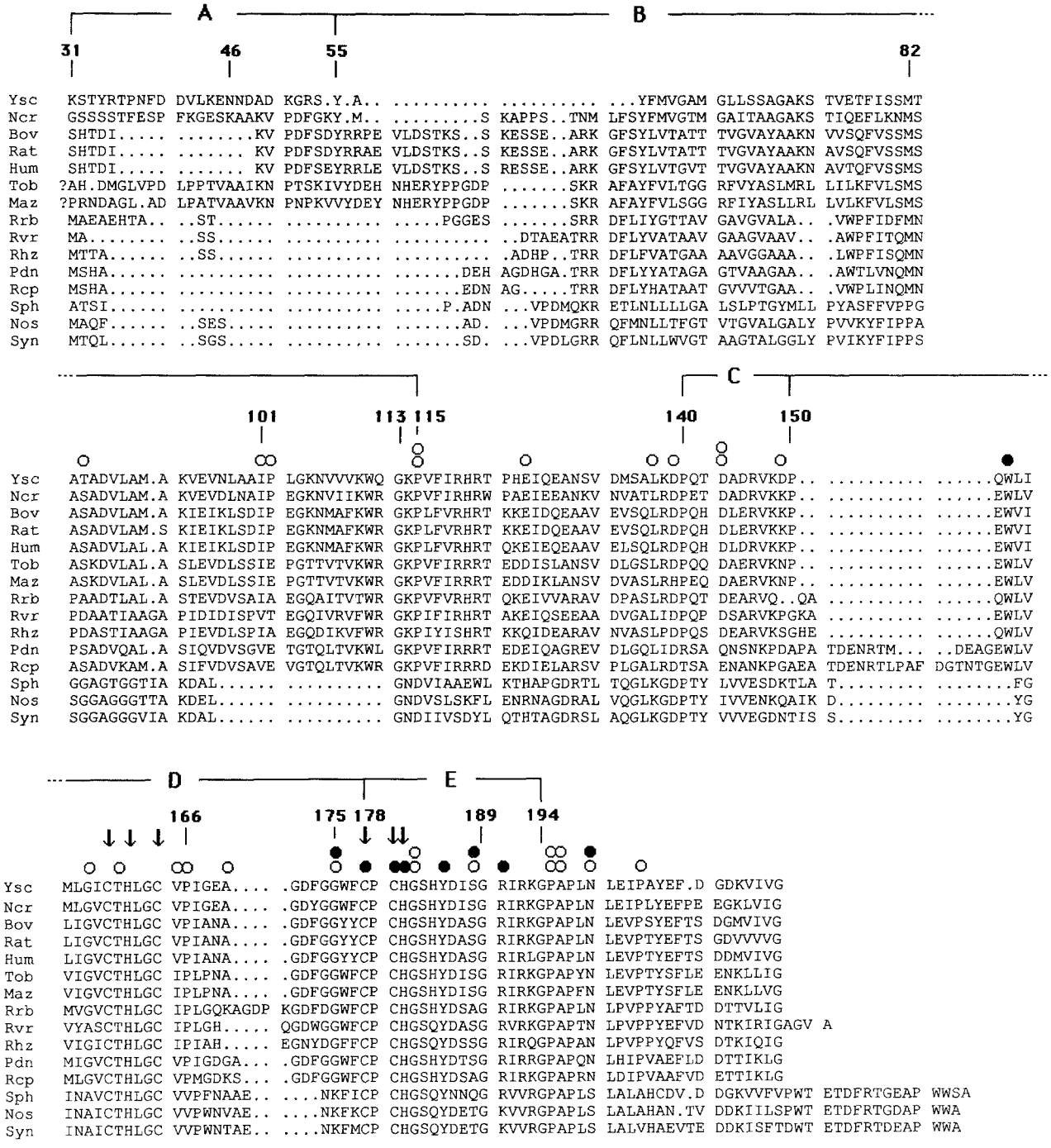

Fig. 1. Alignment of amino acid sequences of iron–sulfur proteins from phylogenetically diverse species, showing conserved structural domains, location of possible iron–sulfur cluster ligands, and the location of temperature-sensitive petite and petite mutations in the *S. cerevisiae* iron–sulfur protein. The numbers above the sequences refer to the amino acids which delineate the five structural domains and subdomains therein which are conserved in the Rieske protein throughout all species. The numbers correspond to the position of the amino acids in the *S. cerevisiae* protein, and are shown against the predicted secondary structure of the *S. cerevisiae* protein in Fig. 3. The five conserved structural domains are designated A through E, and are delineated above the sequences. Arrows point to the amino acids which are possible ligands to the iron–sulfur cluster. Open circles indicate loci of temperature-sensitive petite mutations, and solid circles indicate loci of petite mutations in the yeast protein. Abbreviations for the various species and references to the published sequences are in the text.

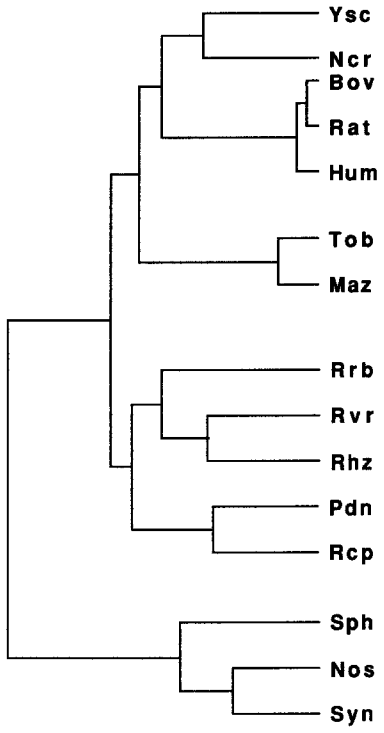

Fig. 2. Sequence similarity relationships among the iron–sulfur proteins of various species as deduced from amino acid sequences. The dendrogram was constructed with the "PILEUP" algorithm in the GCG software collection. The dendrogram is not a phylogenetic reconstruction, although the lengths of the vertical branches are proportional to the similarity between the sequences.

Cys-178 is located an appropriate distance from His-181 to function as a ligand, and is separated from His-161 and the two remaining conserved cysteines by a flexible domain which is conserved in all species. We thus deduce that Cys-178 is one of the two cysteine ligands.

We initially speculated that Cys-164 was the second sulfur ligand (Beckmann *et al.*, 1989). Our reasoning was that a temperature-sensitive mutation proximal to Cys-159, in which Gly-157 was changed to a more electronegative serine, did not eliminate iron–sulfur cluster function and diminished cytochrome *c* reductase activity at permissive temperature only 50%. Recently, after a more extensive mutagenesis of the cloned RIP1 gene, we isolated a second temperature-sensitive mutant, in which Thr-160 is changed to alanine, which eliminates an electronegative residue proximal to Cys-159. This change has almost no effect on cytochrome *c* reductase activity at permissive temperature (Fig. 4). In contrast, a temperature-sensitive mutant proximal to Cys-164, in which Pro-166 was converted to serine, reduced the cytochrome *c* reductase activity at permissive temperature to less than 20% of the wild-type activity. While exchange of an adjacent hydrophobic residue to another (Val-165 to alanine) had very little effect on cytochrome *c* reductase activity at permissive temperature. We thus still favor our initial speculation that the four iron–sulfur cluster ligands are His-161, His-181, Cys-164, and Cys-178 (Fig. 3), rather than Cys-159, as proposed by Davidson *et al.* (1992).

The only region of the iron–sulfur protein in which there is 100% conservation of amino acid sequence throughout all of the species are two hexapeptides encompassing the four conserved cysteines and two histidines in the carboxyl one-third of the protein. In the yeast protein the first of these conserved peptides begins with C-159 and includes the sequence CTHLGC (Fig. 1). The second conserved peptide begins with C-178, and includes the sequence CPCHGS. Although these are the only 100% conserved sequences, there is extensive sequence homology in the carboxyl one-third of the protein, in which one hydrophobic amino acid is exchanged for another.

Even though there is little sequence identity among the various iron–sulfur proteins, a comparison of the predicted secondary structures of the 15 proteins listed in Fig. 1 reveals that there are several highly conserved features in the structures of these proteins. One notable feature of the iron–sulfur proteins is that they contain an extensive number of flexible domains, and they are generally lacking in conserved α helices or β pleated sheets. Of the 185 amino acids in the mature yeast iron–sulfur protein, 14% are glycine (17 residues) or proline (11 residues).

In all of the iron–sulfur proteins thus far sequenced, it is possible to recognize five structural domains which are conserved. The arrangement of these five domains along the length of the protein is depicted by a "horizontal domain map" on the bottom of Fig. 3. The boundaries of these domains are shown on the secondary structure of the yeast iron–sulfur protein (Fig. 3) and above the sequence alignments (Fig. 1). The N-terminal half of the iron–sulfur proteins is distinguished by a bipartite structure, in which a hydrophilic domain (A) is followed by a long hydrophobic domain (B). This hydrophobic domain includes at least one extended α helix in all of the species, and is flanked by two hydrophilic flexible regions, shown by the solid black areas on the domain map in Fig. 3.

The carboxyl one-third of the iron–sulfur proteins is composed of three conserved domains which

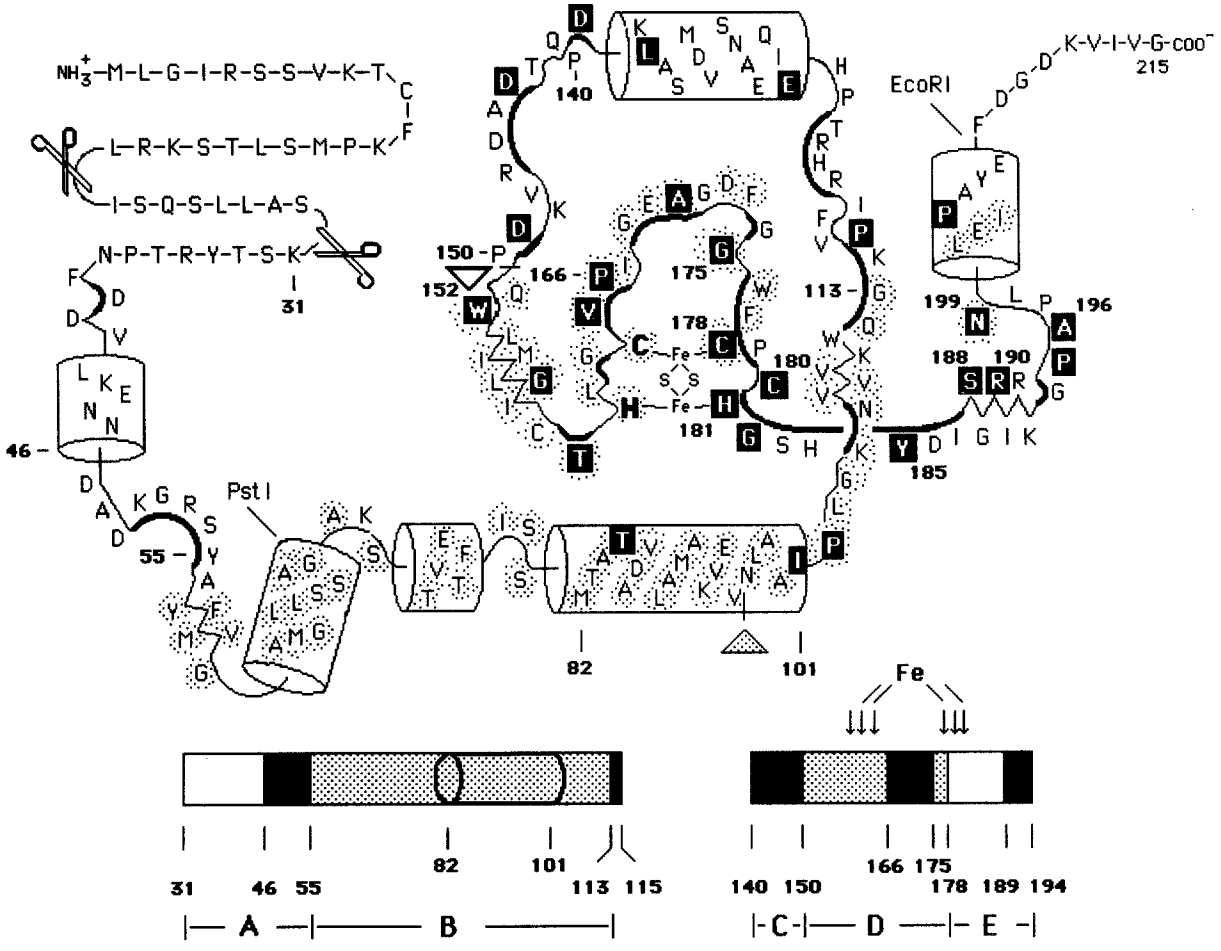

Fig. 3. Predicted secondary structure of the Rieske iron–sulfur protein of *S. cerevisiae* showing the locations of temperature-sensitive petite and petite mutations. Amino acids which are loci of mutations are enclosed in a black box; those which are loci of mutations which gave rise to immunologically detectable iron–sulfur protein but complete lack of growth of the yeast on nonfermentable carbon sources are indicated by a number beside the black box. The scissors indicates the two sites of post-translational processing of the iron–sulfur protein by mitochondrial proteases. Hydrophobic regions of the protein are indicated by stipling around the amino acids. The stipled triangle indicates the region in the sequence of the yeast iron–sulfur protein where there is a deletion of approximately 15 amino acids in the sequences of the iron–sulfur proteins from spinach, *Nostoc*, and *Synechococcus*. The inverted open triangle indicates the region in the sequence of the yeast iron–sulfur protein where there is an insertion of 10–15 amino acids in the iron–sulfur proteins from *P. denitrificans* and *Rh. capsulatus*. Below the predicted secondary structure is shown a horizontal map of the five structural domains (A–E) which are conserved in the iron–sulfur proteins throughout all species. Clear areas on the map indicate hydrophilic domains; solid black areas indicate flexible, hydrophilic domains; stipled areas on a clear background indicate hydrophobic domains; and stipled black areas indicate flexible hydrophobic domains. Arrows above the map point to approximate locations of the possible ligands to the iron–sulfur cluster.

provide a hydrophobic environment wrapped around the iron–sulfur cluster. The first of these three domains (C) is an extended hydrophilic flexible region. This flexible domain is flanked by two prolines (Pro-140 and Pro-150) in the yeast protein. This domain is predicted to be in a hydrophilic region of the bc_1 complex, exposed to an aqueous interface, since the hydrophilic, flexible structure of the domain is conserved, but the amino acid sequence is not. Consistent with the possible solvation of this hydrophilic flexible domain is the finding that three temperature-sensitive mutants were isolated in this region, in which the acidic charge on an aspartic acid was eliminated by the mutation (Figs. 3 and 4).

Table I. Site-Directed Mutations of Conserved Cysteines and Histidines Considered as Possible Ligands to the Iron–Sulfur Cluster in the Rieske Iron–Sulfur Protein

Amino acid	Mutant allele	Growth phenotype
Cys-159	Ser	Petite
Cys-159	Ala	?
His-161	Arg	Petite
His-161	Cys	?
Cys-164	Ser	Petite
Cys-164	Ala	?
Cys-178	Ser	Petite
Cys-178	Ala	Petite
Cys-180	Ser	Petite
Cys-180	Ala	Petite
His-181	Arg	Petite
His-181	Cys	Petite
His-184	Arg	Normal
His-161 and His-181	Cys and Cys	Petite

The middle domain (D) in the carboxyl terminus is hydrophobic and includes a highly flexible, hydrophobic region. In the yeast protein this flexible region extends from Pro-166 to Gly-175, and five of the ten amino acids are prolines or glycines. The third of the carboxyl terminal domains (E) is hydrophilic, and terminated by a short flexible region. We speculate that the flexible E domain allows the distal carboxyl terminus of the protein to fold inward, possibly "capping" an envelope which contains the iron–sulfur cluster. The arrangement of the iron–sulfur cluster ligands within domains C, D, and E is such that two of the ligands, His-161 and one of the cysteines, are buried within the hydrophobic interior of domain D in all of the species. The remaining two ligands, His-181 and one of the cysteines, are at the interface between the hydrophobic domain D and the hydrophilic domain E.

The effect of this positioning of the cluster ligands is that the iron–sulfur cluster is inserted into a hydrophobic region of the protein, with one edge exposed to a hydrophilic environment, and the cluster-sequestering region of the protein is flanked by two very flexible regions at each end, domain C and the terminus of domain E. In addition, the four ligands to the iron–sulfur cluster are bifurcated by the highly flexible hydrophobic region in domain D, with the consequence that the portion of the protein between the two 100% conserved hexapeptides can be folded in a manner to allow the cluster to form a bridge within this relatively short region of polypeptide as shown in Fig. 3.

ISOLATION OF MUTANTS OF THE *S. CEREVISIAE* RIESKE IRON–SULFUR PROTEIN

In order to investigate structure/function relationships in the Rieske iron–sulfur protein, we set up a system for mutational analysis of the protein (Beckmann *et al.*, 1989). We constructed a stable yeast deletion strain, JPJ1, in which the chromosomal copy of the iron–sulfur protein gene, RIP1, was displaced by the yeast LEU2 gene. Into this deletion strain we then introduced plasmids carrying copies of RIP1 which had been randomly mutagenized by passage through an *E. coli* mutator strain. The resulting RIP1 mutants can thus be stably propagated, and are not susceptible to high-frequency reversion, as would be the case if a disrupted copy of RIP1 remained in the chromosome, and could be used as a template to correct point mutations in the plasmid-born copy of the gene.

A second key feature of this mutational analysis system is that the plasmid which carries the RIP1 gene is constructed in such a manner that the gene is conveniently divided into two pieces by digestion with unique restriction enzymes (Beckmann *et al.*, 1989). Digestion with HindIII and PstI excises a segment of the RIP1 gene, including the upstream elements necessary for its expression and a portion of the coding region corresponding to the N-terminus of the protein, including the cleavable presequence and domain A of the mature protein. The location of this PstI site at the beginning of domain B is shown in Fig. 3. Digestion of the plasmid-born RIP1 with PstI and EcoRI liberates the remainder of the mature protein, except for nine amino acids at the carboxyl terminus.

The design of this plasmid thus allows mutagenesis of the RIP1 gene in *E. coli* followed by screening for mutant phenotypes in yeast. When mutant RIP1 genes are thus confirmed, the gene can be conveniently dissected into two fragments by transferring the two restriction fragments into a wild-type copy of the plasmid-born RIP1 in which the corresponding fragment is deleted. In this manner it is possible to quickly localize the site of a suspected point mutation to a fragment of the RIP1 gene which is sufficiently short that it can be sequenced in its entirety by one or two sequencing runs.

We thus mutagenized the plasmid-born RIP1 by passage through an *E. coli* mutator strain (Beckmann *et al.*, 1989; Graham and Trumpower, 1991), and screened the plasmids in JPJ1 for mutants which

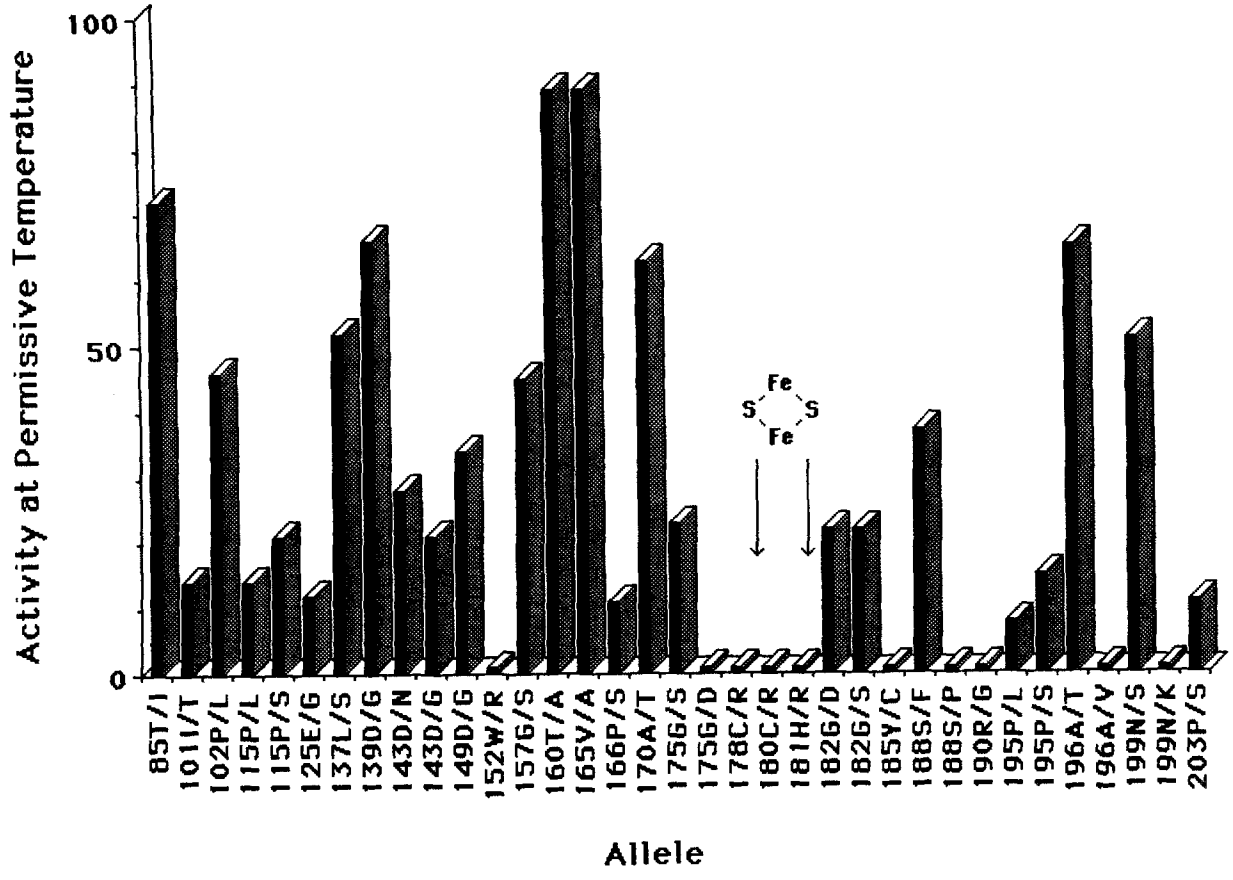

Fig. 4. Ubiquinol-cytochrome *c* reductase activities of iron–sulfur protein mutants at permissive temperatures. Mitochondrial membranes were isolated from yeast grown at permissive temperature (23°C) on galactose, and ubiquinol-cytochrome *c* reductase activities measured at the same temperature. Numbers below the graph identify the wild-type and mutant alleles of the various iron-sulfur protein mutants. Activities are expressed as percentages of the activity measured with mitochondrial membranes from the parental strain (W303-1A) grown under the same conditions.

exhibited temperature-sensitive growth on nonfermentable carbon sources, or which failed to grow on nonfermentable carbon sources but which possessed immunologically detectable iron–sulfur protein. We obtained 100 independently isolated RIP1 mutants, which were then submitted to gene dissection, after which the segment of the gene carrying the mutant allele was sequenced.

After sequencing the 100 independently isolated mutants, we identified 25 mutant alleles which exhibited temperature-sensitive growth on ethanol/glycerol ("temperature sensitive petites") and 10 mutant alleles which failed to grow on ethanol/glycerol ("petites"), but which synthesized iron–sulfur protein in sufficient quantities and of sufficient stability that it could be detected on PAGE-SDS by Western analysis of the mitochondrial membranes from those mutants. Several of the mutant alleles were isolated multiple times. The RIP1 genes carrying the 35 unique mutant alleles were then subcloned into single-copy plasmids and transformed into JPJ1 for further biochemical characterization (Ljungdahl *et al.*, 1989).

All of the mutants obtained in this extensive screen had point mutations in the portion of the gene flanked by the PstI and EcoRI restriction sites, as shown in Fig. 3. The location of the mutant alleles is shown above the aligned sequences in Fig. 1, and the cytochrome *c* reductase activities of the mitochondrial membranes from the yeast containing single copies of the mutant gene and grown at permissive temperature are shown in Fig. 4. Three of the temperature-sensitive mutations reside in the hydrophobic domain B. One of these, 85T/I, alters the sensitivity of the bc_1 complex to an inhibitory analogue of ubiquinone, and is thus

suspected of being proximal to the site where the iron–sulfur protein binds ubiquinol (Ljungdahl *et al.*, 1989). The two remaining mutations in domain B interfere with post-translational processing of the iron–sulfur protein, as discussed below.

The remaining 32 mutations all fall within the carboxyl half of the protein, and most of these reside within what we predict is the central "core" of the protein. All of the mutations fall on amino acids which are extensively conserved throughout the species (Fig. 1), although not universally, as might be expected if conservation reflects an essential role of an amino acid. Interestingly, we did not obtain any point mutations in the N-terminus of the protein, which might be expected to block import or post-translational processing of the protein, although a more extensive mutagenesis might do so.

Many of the mutant alleles exhibit phenotypes which are not unexpected. For example, 178C/R, 180C/R, and 181H/R introduce charged arginines in place of or proximal to the iron–sulfur cluster ligands, and the resulting iron–sulfur proteins are completely inactive. Similarly the 160T/A, 165V/A, and 179A/T mutations involve relatively conservative exchanges and have relatively small effects on the cytochrome *c* reductase activities (Fig. 4).

In some cases different mutant alleles of the same amino acid gave rise to different phenotypes. Conversion of Gly-175 to serine resulted in a temperature-sensitive iron–sulfur protein, while conversion of the same glycine to an aspartate resulted in an inactive iron–sulfur protein at any temperature. This difference between temperature-sensitive and inactive alleles is seen more dramatically at Ala-196. Conversion of Ala-196 to threonine has a modest effect on activity, while what would be an expected conservative change of the same alanine to a valine results in an inactive protein. A similar difference of temperature-sensitive alleles is seen at Gln-199 (Fig. 4). Changing Gln-199 to lysine eliminates iron–sulfur protein activity, while changing Gln-199 to serine has only a modest effect on iron–sulfur protein activity. The latter change occurs naturally in the photosynthetic species, where serine is normally present at this position (Fig. 1).

An unexpected outcome of the mutational analysis was the finding that the extreme carboxyl terminus of the protein appears to be especially sensitive to mutational alterations in function. Ten mutants were isolated in the section of sequence beginning with Ser-188, and four of these were inactive (Fig. 3). This finding is the basis for our prediction that the flexible region at the carboxyl terminus of domain E folds into the protein and performs an essential structural role in maintaining the redox capabilities of the iron–sulfur cluster.

The identification of these randomly generated mutations is an informative starting point from which we can now design site-directed mutagenesis. We have begun such experiments by first making site-directed mutants of the four conserved cysteines and two conserved histidines, with the objective of defining which are the ligands to the iron–sulfur cluster. We have additionally constructed a site-directed mutation of His-184, which is conserved in the iron–sulfur proteins from most of the oxygenic species, but which is converted to a glutamine in four of the photosynthetic organisms and rhizobia (Fig. 1). Conversion of His-184 to arginine by site-directed mutagenesis in yeast did not impair iron–sulfur protein function (Graham and Trumpower, 1991).

The current status of the site-directed mutations of the suspected iron–sulfur cluster ligands is summarized in Table I. All of the mutations introduced and characterized thus far have resulted in loss of iron–sulfur protein function. However, two of the potentially most informative mutations, converting Cys-159 and Cys-164 to alanines, are not yet fully characterized. Likewise, although we know that simultaneously converting His-161 and His-181 to cysteines eliminates iron–sulfur protein function, we do not yet know whether this conversion has resulted in the formation of a classical ferredoxin-like iron–sulfur cluster, which was the intent of the site-directed mutagenesis.

IMPORT AND POST-TRANSLATIONAL PROCESSING OF THE RIESKE IRON–SULFUR PROTEIN

Import of the Rieske iron–sulfur protein is accompanied by two post-translational protease processing events in mitochondria from *N. crassa* (Hartl *et al.*, 1986) and *S. cerevisiae* (Cheng *et al.*, 1989; Japa and Beattie, 1989). In yeast the matrix-processing protease (MPP) initially removes a 22 amino acid presequence to convert the precursor iron–sulfur protein (p-ISP) to intermediate sized iron–sulfur protein (i-ISP). A second protease, the mitochondrial intermediate protease (MIP), then removes an octapeptide to form mature sized iron–sulfur protein (m-ISP).

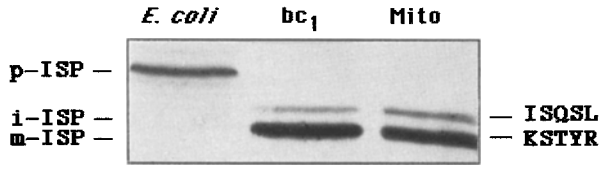

Fig. 5. Western blot analysis of cytochrome bc_1 complex separated by PAGE-SDS showing intermediate sized iron–sulfur protein (i-ISP) and mature sized iron–sulfur protein (m-ISP) in the purified cytochrome bc_1 complex. The lane on the left shows the migration position of precursor iron–sulfur protein (p-ISP) synthesized off a plasmid in *E. coli*. The lane in the middle shows the intermediate and mature sized iron–sulfur protein in cytochrome bc_1 complex purified from the parental yeast strain, W303-1A. The lane on the right shows the intermediate and mature sized iron–sulfur protein in mitochondrial membranes from the same yeast strain. Iron–sulfur protein was located after trans-blotting by probing with a monoclonal antibody. To the right of the gel are shown the first five amino acids in the N-terminal sequences of the intermediate and mature sized iron–sulfur proteins, obtained by gas-phase sequencing of the proteins in the purified bc_1 complex.

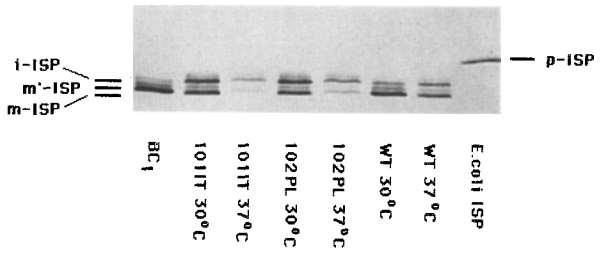

Fig. 6. Temperature-sensitive mutations in the mature portion of the iron–sulfur protein which block processing of i-ISP to m-ISP. The figure shows Western blot analysis of mitochondrial membranes from the W303-1A parental strain (WT) and of two temperature-sensitive mutants (101IT and 102PL) separated by PAGE-SDS and probed with monoclonal antibodies to the iron–sulfur protein. Purified cytochrome bc_1 complex is shown in the left lane, and precursor iron–sulfur protein synthesized in *E. coli* is shown in the right lane. The migration positions of iron–sulfur protein precursor (p-ISP), intermediate sized iron–sulfur protein (i-ISP), and mature sized iron–sulfur protein (m-ISP) are marked, as is the migration position of a fourth, unidentified form of the iron–sulfur protein (m′-ISP).

These two protease-processing sites are shown by scissors in Fig. 3.

We have found that conversion of i-ISP to m-ISP occurs after i-ISP is in the cytochrome bc_1 complex in yeast. Evidence for this is shown in Fig. 5, which shows the presence of i-ISP in purified bc_1 complex. To confirm that this protein band in the purified bc_1 complex is indeed i-ISP, and not a coincidental artifactual migration of m-ISP, we separated the suspected i-ISP and m-ISP proteins by PAGE-SDS and submitted the two proteins to five cycles of N-terminal amino acid sequencing. The sequences of the first five amino acids of the two proteins are shown to the right of the Western blot. These two sequences match exactly the sequences expected for the N-termini of i-ISP and m-ISP.

For comparison we have also shown the migration of p-ISP, synthesized in *E. coli*, and the migration positions of i-ISP and m-ISP in mitochondrial membranes. It is notable that the ratio of i-ISP to m-ISP is essentially identical in the purified bc_1 complex and the mitochondrial membranes, indicating that all of the intermediate sized iron–sulfur protein present in mitochondria is present in the bc_1 complex. We have never detected p-ISP in yeast mitochondria, suggesting that the rate of conversion of p-ISP to i-ISP under steady-state growth conditions is rapid, and that the endogenous pool of p-ISP is undetectably small.

Two temperature-sensitive point mutations in the mature portion of the iron–sulfur protein block conversion of i-ISP to m-ISP. These two mutations, conversion of Ile-101 to threonine and conversion of Pro-102 to leucine, both reside in domain B, at the end of the hydrophobic helix. Accumulation of i-ISP at 30 and 37°C in the 101I/T and 102 P/L mutants is shown in Fig. 6. In mitochondrial membranes from both the mutants and the parental strain we observed a small amount of iron–sulfur protein species which migrates between i-ISP and m-ISP. We have labeled this species as m′-ISP, since sequencing of this species along with i-ISP and m-ISP which were separated by PAGE-SDS indicated that m′-ISP has an amino terminal sequence identical to that of m-ISP. Whether m′-ISP is truly a distinct species of iron–sulfur protein, or an electrophoresis artifact, remains to be established. The presence of this unidentified form of iron–sulfur protein caused us to erroneously assume that the three forms of iron–sulfur protein seen *in vivo* were p-ISP, i-ISP, and m-ISP (Beckmann *et al.*, 1989). That this is not the case is shown by the migration position of the true p-ISP, translated in *E. coli*, as shown in the lane on the right side of the gel in Fig. 6.

It is interesting to speculate how these two mutations might block processing of i-ISP to m-ISP when they are separated from the MIP cleavage site by 70 amino acids. It has been generally thought that MIP cleavage occurs from the matrix side of the inner mitochondrial membrane (Hartl *et al.*, 1986; Cheng *et al.*, 1989; Hendrick *et al.*, 1989), while the known

function of the iron–sulfur protein requires that it be located toward the exterior side of the inner mitochondrial membrane (Trumpower, 1990a,b). Examination of the predicted secondary structure of the iron–sulfur protein indicates that the protein is probably anchored to the bc_1 complex by a transmembranous hydrophobic domain in the amino terminal half of domain b. If these assumed topologies are correct, it would require that point mutations at Ile-101 and Pro-102 must transmit a structural change through the membrane, to the site of protease cleavage. One way in which this could occur would be if the MIP cleavage site is close to the matrix surface of the inner membrane and the mutations on the opposite side of the membrane cause the distal amino terminus of the protein to be withdrawn further into the membrane such that MIP cleavage is sterically hindered.

As noted above, post-translational processing of iron–sulfur protein proceeds in two steps in *N. crassa* and *S. cerevisiae*. Examination of the N-terminal sequences shown in Fig. 7 indicates that sites for MPP and MIP cleavage also exist in the *Sc. pombe* iron–sulfur protein, which was cloned and sequenced in this laboratory recently (J. P. di Rago, L. A. Graham, and B. L. Trumpower, unpublished results). However, in the iron–sulfur proteins from bovine, rat, and human mitochondria the MPP cleavage site is located at a position which would generate m-ISP, rather than i-ISP, in those species. In other words, although the iron–sulfur protein is processed in two steps in lower eukaryotes, it appears likely that it is processed in a single step in mammals. Our recent studies on the *in vitro* processing of bovine p-ISP by rat-liver mitochondria have shown that this is indeed the case (Brandt *et al.* 1993): The presequence of the bovine ISP is removed in a single step and identical to subunit 9 of the cytochrome bc_1 complex.

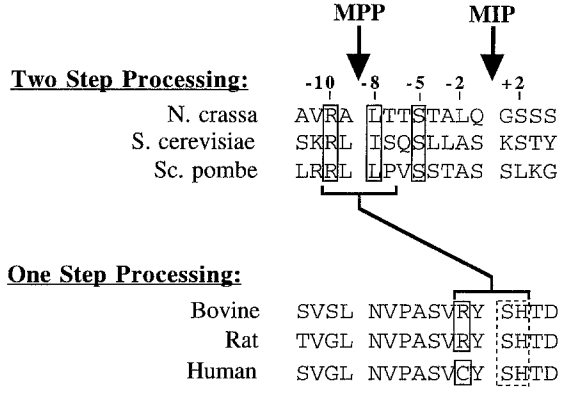

Fig. 7. N-terminal amino acid presequences of the iron–sulfur proteins from lower and higher eukaryotes, showing known and predicted sites of post-translational protease processing. The arrows point to the known or predicted sites of processing by the matrix processing protease (MPP) or mitochondrial intermediate protease (MIP). Numbers refer to positions of the amino acids, with the N-terminus of the mature iron–sulfur proteins being number 1. The boxes indicate the consensus sequence motif for two-step processing according to Hendrick *et al.* (1989).

INVOLVEMENT OF THE 7.3-kDa SUBUNIT 9 IN INSERTION OF IRON–SULFUR CLUSTER INTO THE IRON–SULFUR PROTEIN IN *S. CEREVISIAE*

We previously reported the construction of a deletion mutant of *S. cerevisiae*, JDP1, in which the nuclear gene which encodes the 7.3-kDa subunit 9 of the yeast cytochrome bc_1 complex was replaced by a selectable marker (Phillips *et al.*, 1990). This deletion mutant has a temperature-dependent respiratory petite phenotype, although optical spectra indicate that a spectrally detectable cytochrome bc_1 complex is assembled. To understand how the presumed loss of a single polypeptide, itself lacking a redox prosthetic group, leads to loss of ubiquinol-cytochrome *c* reductase activity, we have further characterized the cytochrome bc_1 complex in JDP1 (Graham *et al.*, 1992).

The traces in Fig. 8 show reduction of cytochrome *b* by menaquinol in mitochondrial membranes from the parental and subunit 9 deletion strains. Menaquinol reduces a greater extent of the cytochrome *b* than does ubiquinol, owing to its more negative oxidation–reduction potential, and can reduce the cytochrome through either center N or center P. Thus, in the absence of any inhibitors, menaquinol reduces cytochrome *b* in both the wild-type and the subunit 9 deletion strains, as shown by the top two tracings in Fig. 8.

The two middle traces in Fig. 8 show reduction of cytochrome *b* when electron transfer through center N is blocked by antimycin. Under these conditions cytochrome *b* reduction proceeds through center P in the wild-type bc_1 complex. However, in the presence of antimycin there is no reduction of cytochrome *b* through center P in the bc_1 complex lacking subunit 9.

If electron transfer through center P is blocked by methoxyacrylate-stilbene, cytochrome *b* is reduced through center N (Brandt *et al.*, 1988). This pathway of cytochrome *b* reduction remains operative when subunit 9 is deleted, as can be seen by comparing the bottom right and top right tracings in Fig. 8. The

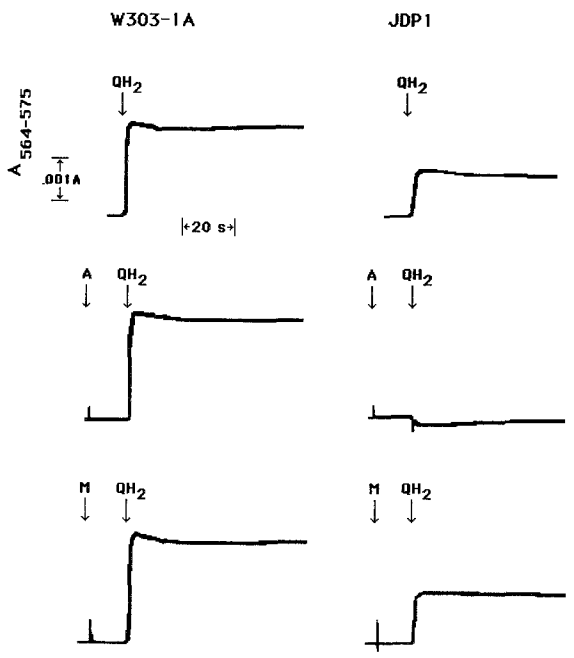

Fig. 8. Loss of iron–sulfur protein-catalyzed cytochrome *b* reduction through the center P ubiquinol oxidase site in the absence of subunit 9. The tracings show pre-steady-state reduction of cytochrome *b* by menaquinol in mitochondrial membranes from yeast in which subunit 9 of the cytochrome bc_1 complex is present or absent, and the effects of bc_1 complex inhibitors on reduction of cytochrome *b*. The tracings on the left are of cytochrome *b* reduction in the parental strain (W303-1A), and those on the right are of cytochrome *b* reduction in the subunit 9 deletion strain (JDP1). The arrows show additions of menaquinol (QH_2), antimycin (A), or methoxyacrylate-stilbene (M).

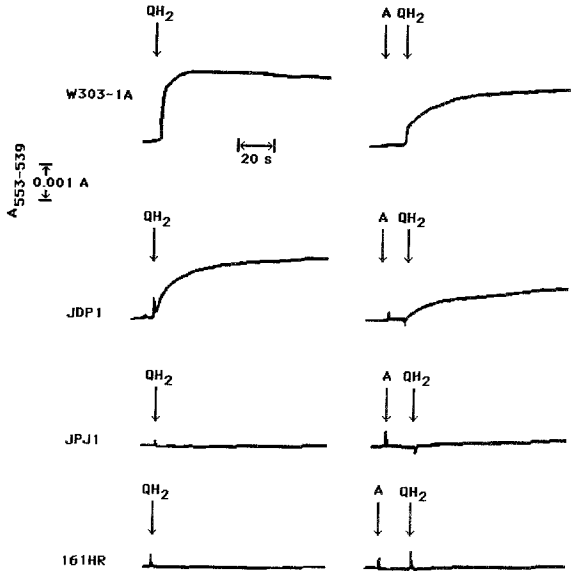

Fig. 9. Loss of iron–sulfur protein-catalyzed cytochrome c_1 reduction through the center P ubiquinol oxidase site in the absence of subunit 9. The tracings on the left show reduction of cytochrome c_1 by ubiquinol (QH_2) in mitochondrial membranes prepared from the parental yeast strain, W303-1A; the subunit 9 deletion, JDP1; the iron–sulfur protein deletion strain, JPJ1; and a site-directed mutant strain, 161HR. The tracings on the right show reduction of cytochrome c_1 in the same strains in the presence of the inhibitor antimycin (A).

amount of cytochrome *b* reduced by menaquinol in the subunit 9 deletion strain, either in the absence of inhibitors or in the presence of methoxyacrylate-stilebene, is about 60% of that in the wild-type cytochrome bc_1 complex. This decrease in cytochrome *b* reduction is partly due to reoxidation of the menaquinol-reduced cytochrome *b* which occurs in the absence of subunit 9, which was confirmed by optical spectra taken at intervals after reduction of cytochrome *b* by menaquinol (results not shown). In addition, it is possible that the lack of subunit 9 either specifically damages the heme of b-566 or breaks electronic communication between the two hemes, such that in the absence of electron transfer through center P there is no route for reduction of the low-potential b-566.

The tracings in Fig. 9 show cytochrome c_1 reduction by ubiquinol through center P, in mitochondrial membranes from the parental (W303-1A) and subunit 9 deletion strains (JDP1). In the parental strain c_1 reduction is so rapid that the rate ($t_{1/2} < 100$ msec) is masked by the mixing time (1 sec) of the spectrophotometer. In the subunit 9 deletion strain the rate of cytochrome c_1 reduction, shown in the second trace on the left, is markedly slowed, having a half-time in excess of 10 sec. This result also suggests that electron transfer through center P is impaired in JDP1 (Edwards *et al.*, 1982).

Optical spectra taken after reduction of the bc_1 complex by ubiquinol show that ubiquinol also elicits oxidant-induced cytochrome *b* reduction in the parental strain (Bowyer *et al.*, 1981), resulting in an absorption peak at 562 nm. This oxidant-induced cytochrome *b* reduction is not observed after ubiquinol reduction of the bc_1 complex in the subunit 9 deletion strain (results not shown), confirming that electron transfer through center P is impaired in the absence of subunit 9. Under the conditions of the experiments in Fig. 9 there is virtually no reduction of cytochrome *b* via center N, owing to the relatively high potential of the ubiquinol substrate, which is further increased by oxidation of ubiquinol by cytochrome c_1.

When antimycin is added to the wild-type complex, reduction of c_1 occurs with an initial rapid phase,

followed by a slower reaction which proceeds on a time scale of seconds, shown by the top right trace in Fig. 9. This biphasic reduction results from relatively similar midpoint potentials of cytochrome c_1 and iron–sulfur protein (Rich, 1983) with the result that the first electron from ubiquinol equilibrates between these two redox centers rapidly, since antimycin does not inhibit the first turnover of the bc_1 complex (Bowyer and Trumpower, 1981). Antimycin inhibits reoxidation of cytochrome *b* and the second and subsequent turnovers of the complex, thus introducing a slow phase into the rate of cytochrome c_1 reduction in the yeast bc_1 complex.

In the absence of subunit 9 antimycin eliminates the rapid phase of c_1 reduction, as shown by the second trace in the right column (Fig. 9). Reduction of cytochrome c_1 becomes monotonic, and is slower than in the deletion strain in the absence of the inhibitor. This effect of antimycin on the subunit 9 deletion complex is likely due to a conformational change at the center P ubiquinol oxidase site which is magnified in the absence of subunit 9. Antimycin is known to cause a conformational change in the cytochrome bc_1 complex, resulting in a loosening of the Rieske iron–sulfur protein (Rieske *et al.*, 1967; Rieske, 1976). We attribute the inhibitory effect of antimycin on cytochrome c_1 reduction in the subunit 9 deletion strain to a more extreme loosening of the Rieske iron–sulfur protein from the bc_1 complex, resulting in the more extensive lowering of the rate of electron transfer to cytochrome c_1.

Although cytochrome c_1 reduction is slowed by the absence of subunit 9, it is not completely blocked. For comparison, we have included tracings showing that cytochrome c_1 reduction is completely absent if iron–sulfur protein is deleted. The difference in rates of cytochrome c_1 reduction in JDP1, the subunit 9 deletion strain, and JPJ1, the iron–sulfur protein deletion strain, is consistent with the very slow growth of JDP1 on nonfermentable carbon sources at room temperature (Phillips *et al.*, 1990), and the complete lack of growth of JPJ1 on similar substrates at any temperature (Beckmann *et al.*, 1987). The bottom left trace in Fig. 9 shows reduction of cytochrome c_1 in membranes from an iron–sulfur protein mutant, 161HR, in which the iron–sulfur apoprotein is processed to its mature size and assembled into the bc_1 complex, but the iron–sulfur cluster is not inserted (Graham and Trumpower, 1991). Mature size iron–sulfur apoprotein cannot catalyze slow cytochrome c_1 reduction of the type seen in JDP1.

Western blot analysis of the mitochondrial membranes from JDP1 indicated that immunologically detectable iron–sulfur protein is present in normal amounts when subunit 9 is deleted, but the protein is more sensitive to degradation by endogenous proteases. When these same membranes were examined by low-temperature EPR spectroscopy, we discovered that the signature *g* 1.90 resonance of the Rieske iron–sulfur cluster is not detectable in JDP1, even though mature size apoprotein is present (results not shown).

There are two possible explanations for the slow reduction of cytochrome c_1 seen in JDP1. One possibility is that a normally assembled iron–sulfur cluster is present in a small percentage of the bc_1 complexes, and that cytochrome c_1 is rapidly reduced in these complexes, after which there is slow electron transfer between cytochrome c_1's in active and inactive complexes. Such a small subset of complexes could account for the low ubiquinol-cytochrome *c* reductase activity (less than 5% of the wild-type) which is observed in JDP1, and the corresponding percent of cytochrome c_1 which would be rapidly reduced would be too low to be resolved from the bulk of the slowly reacting cytochrome c_1. Similarly, it is possible that we would not detect an EPR signal from the Rieske center if less than 5% of the centers have a native cluster.

A second possibility is that all of the bc_1 complexes contain a Rieske protein possessing a partially assembled and EPR-silent derivative of the iron–sulfur cluster. Such a derivative iron protein could be redox active, but react sluggishly. We conducted experiments which suggest that the latter explanation is probably correct. We added a limiting amount of methoxyacrylate-stilbene, such that cytochrome c_1 reduction was inhibited in approximately 50% of the bc_1 complexes of the parental membranes. Following rapid reduction of cytochrome c_1 in the noninhibited population of complexes, there was virtually no slow reduction of the cytochrome c_1 in the remainder of the complexes. In other words, there appears to be no lateral electron transfer between complexes at the level of cytochrome c_1.

This interpretation was further confirmed by examining the effect of methoxyacrylate-stilbene on cytochrome c_1 reduction in membranes from JDP1. When a substoichiometric amount of methoxyacrylate-stilbene was added to the JDP1- membranes, the initial slow rate of cytochrome c_1 reduction ensued in some of the bc_1 complexes, but the inhibitor completely blocked cytochrome c_1 reduction in the remainder of

the population (results not shown). This experiment establishes that there is no lateral electron transfer between bc_1 complexes at the level of cytochrome c_1 when subunit 9 is deleted.

Deletion of subunit 9 alters the conformation of the Rieske iron–sulfur protein such that the iron–sulfur cluster is not inserted properly. Consequently, the iron–sulfur protein appears to contain a center which is capable of sluggish electron transfer from ubiquinol to cytochrome c_1, but which is EPR silent. The resulting slow but detectable rate of presteady-state reduction of cytochrome c_1 is consistent with the low ubiquinol-cytochrome c reductase activity ($< 5\%$), which supports slow growth of JDP1 on nonfermentable carbon sources at room temperature. Site-directed mutants of the Rieske iron–sulfur protein, in which ligands to the iron–sulfur cluster are changed so that the cluster cannot be inserted, are processed to their mature size and inserted into the bc_1 complex, but do not catalyze this slow reduction of cytochrome c_1, have no detectable cytochrome c reductase activity, and do not grow on nonfermentable carbon sources at any temperature (Graham and Trumpower, 1991).

REFERENCES

Beckmann, J. D., Ljungdahl, P. O., Lopez, J. L., and Trumpower, B. L. (1987). *J. Biol. Chem.* **262**, 8901–8909.

Beckmann, J. D., Ljungdahl, P. O., and Trumpower, B. L. (1989). *J. Biol. Chem.* **264**, 3713–3722.

Bowyer, J. R., and Trumpower, B. L. (1981). *J. Biol. Chem.* **256**, 2245–2251.

Bowyer, J. R., Edwards, C. A., and Trumpower, B. L. (1981). *FEBS Lett.* **126**, 93–97.

Brandt, U., Schägger, H., and Von Jagow, G. (1988). *Eur. J. Biochem.* **173**, 499–506.

Brandt, U., Yu, L., Yu, C.-A., Trumpower, B. L. (1993). *J. Biol. Chem.* **268**, 8387–8390.

Britt, R. D., Sauer, K., Klein, M. P., Knaff, D. B., Kriauciunas, A., Yu, C. A., Yu, L., and Malkin, R. (1991). *Biochemistry* **30**, 1892–1901.

Cheng, M. Y., Hartl, F. U., Martin, J., Pollock, R. A., Kalousek, F., Neupert, W., Hallberg, E. M., Hallberg, R. I., and Horwich, A. L. (1989). *Nature (London)* **337**, 620–625.

Davidson, E., and Daldal, F. (1987). *J. Mol. Biol.* **195**, 13–24.

Davidson, E., Ohnishi, T., Atta-Asafo-Adjei, E., Daldal, F. (1992). *Biochemistry* **31**, 3342–3351.

Edwards, C. A., Bowyer, J. R., and Trumpower, B. L. (1982). *J. Biol. Chem.* **257**, 3705–3713.

Graham, L., and Trumpower, B. L. (1991). *J. Biol. Chem.* **266**, 22485–22492.

Graham, L. A., Phillips, J. D., and Trumpower, B. L. (1992). *FEBS Lett.* **313**, 251–254.

Gurbiel, R. J., Batie, C. J., Sivaraja, M., True, A. E., Fee, J. A., Hoffman, B. M., and Ballou, D. P. (1989). *Biochemistry* **28**, 4861–4871.

Harnisch, U., Weiss, H., and Sebald, W. (1985). *Eur. J. Biochem.* **149**, 95–99.

Hartl, F. U., Schmidt, B., Wachter, E., Weiss, H., and Neupert, W. (1986). *Cell* **47**, 939–951.

Hendrick, J. P., Hodges, P. E., and Rosenberg, L. I. (1989). *Proc. Natl. Acad. Sci. USAS* **86**, 4056–4060.

Huang, J., Struck, F., Matzinger, D. F., and Levings, C. S. (1991). *Proc. Natl. Acad. Sci. USA* **88**, 10716–10720.

Japa, S., and Beattie, D. S. (1989). *Arch. Biochem. Biophys.* **268**, 716–720.

Kallas, T., Spiller, S., and Malkin, R. (1989). *Proc. Natl. Acad. Sci. USA* **85**, 5794–5798.

Kuila, D., Fee, J. A., Schoonover, J. R., Woodruff, W. H., Batie, C. J., and Ballou, D. P. (1987). *J. Am. Chem. Soc.* **109**, 1559–1561.

Kurowski, B., and Ludwig, B. (1987). *J. Biol. Chem.* **262**, 13805–13811.

Ljungdahl, P. O., Beckmann, J. D., and Trumpower, B. L. (1989). *J. Biol. Chem.* **264**, 3723–3731.

Majewski, C., and Trebst, A. (1990). *Mol. Gen. Genet.* **224**, 373–382.

Nishikimi, M., Hosokawa, Y., Toda, H., Suzuki, H., and Ozawa, T. (1989). *Biochem. Biophys. Res. Commun.* **159**, 19–25.

Nishikimi, M., Hosokawa, Y., Toda, H., Suzuki, H., and Ozawa, T. (1990). *Biochem. Int.* **20**, 155–160.

Phillips, J. D., Schmitt, M. E., Brown, T. A., Beckmann, J. D., and Trumpower, B. L. (1990). *J. Biol. Chem.* **265**, 20813–20821.

Rich, P. R. (1983). *Biochim. Biophys. Acta* **722**, 271–280.

Rieske, J. S. (1976). *Biochim. Biophys. Acta* **456**, 195–247.

Rieske, J. S., Baum, H., Stoner, C. D., and Lipton, S. HJ. (1967). *J. Biol. Chem.* **242**, 4854–4866.

Schägger, H., Borchart, U., Machleidt, W., Link, T. A., and Von Jagow, G. (1987). *FEBS Lett.* **219**, 161–168.

Steppuhn, J., Rother, C., Hermans, J., Jansen, T., Salnikow, J., Hauska, G., and Hermann, R. G. (1987). *Mol. Gen. Genet.* **210**, 171–177.

Thoeny-Meyer, L., Stax, D., and Hennecke, H. (1989). *Cell* **57**, 683–697.

Trumpower, B. L. (1981). *Biochim. Biophys. Acta* **639**, 129–155.

Trumpower, B. L. (1990a). *Microbiol. Rev.* **54**, 102–129.

Trumpower, B. L. (1990b). *J. Biol. Chem.* **265**, 11409–11412.

Usui, S., Yu, L., and Yu, C. A. (1990). *Biochem. Biophys. Res. Commun.* **167**, 575–579.

Verbist, J., Lang, F., Gabellini, N., and Oesterhelt, D. (1989). *Mol. Gen. Genet.* **219**, 445–452.

Widger, W. R., GenBank Accession No. M74514.